Role of the Ca^{2+}/calmodulin kinase II (CaMKII) and its interaction with the NMDA receptor in homeostatic synaptic plasticity

Tesis Entregada a la Universidad de Chile en Cumplimiento Parcial de los Requisitos para Optar Al Grado de Magíster en Ciencias Biológicas

Facultad De Ciencias

Por

PABLO ISMAEL VERGARA GARCÍA

Julio, 2017

Director de Tesis: Dr. Magdalena Sanhueza Tohá

FACULTAD DE CIENCIAS

UNIVERSIDAD DE CHILE

INFORME DE APROBACION

TESIS DE MAGÍSTER

Se informa a la Escuela de Postgrado de la Facultad de Ciencias que la Tesis de Magister presentada por el candidato

PABLO ISMAEL VERGARA GARCÍA

Ha sido aprobada por la comisión de Evaluación de la tesis como requisito para optar al grado de Magíster en Ciencias Biológicas, en el examen de Defensa Privada de Tesis rendido el día 07 de Julio de 2017.
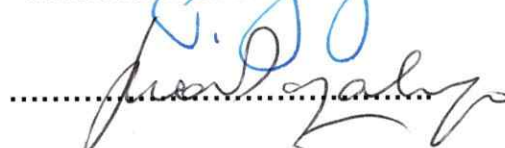
Director de Tesis:

Dra. Magdalena Sanhueza Tohá ....

Comisión de Evaluación de la Tesis:

Dr. Julio Alcayaga Urbina ....

Dr. Juan Bacigalupo Vicuña ....

If the human brain were so simple that we could understand it,

we would be so simple that we couldn't!

Emerson M. Pugh

RESUMEN BIBLIOGRÁFICO

Nací en nochebuena, en el año 1992. Era la única guagua que prefería dormir en vez de comer. He vivido toda mi vida en Santiago. Mis amigos me dicen "Galoy" (se acentúa en la a) por un personaje que cree cuando iba en el colegio, título que cargo hasta estos días. En segundo medio decidí estudiar algo con biología, sin embargo, nunca logré despegar mi cabeza de los números y las humanidades. La verdad es que me gusta todo, y cuando a uno le gusta todo cualquier cosa que uno elija es la elección correcta.

AGRADECIMIENTOS

Las primeras líneas de agradecimiento tienen que ir a mis padres, ya que ellos fueron (son y serán) los factores más determinantes en la formación de mi carácter. Infinito agradecimiento por el soporte incondicional que me han dado.

Agradezco a mis profesores, quienes gentilmente me regalaron sus reflexiones. Agradezco profundamente las conversaciones de pasillo, que a mi parecer hace a mi querida universidad única. Mención honrosa a mi querida tutora, la profe Magda, por dejarme "volar" como científico. Agradezco mucho el cariño de Don Danny y Jeannette, que hacen la vida en el laboratorio tan amena.

Agradecimiento a mis amigos de siempre, por ser de siempre. Como yo sé que quieren ser nombrados, voy a esforzarme (perdón si se me olvida alguno): Va → Rama, Dodo, mari, cony (con éste mato varios pájaros de un tiro), camigu, llama, joacogollo, Toto, Nico, Lean, Don Jorge y xoros del lol (yo sé que esto es trampa, pero no se pueden nombrar todos). A Dontelo Karmelo también le agradezco, pero un poco menos que al resto ya que no me puso en su tesis de doctorado, y le juré venganza.

Finalmente, quiero agradecer a los duendes que me permitieron terminar mi tesis a tiempo y no sabotearon mis experimentos (fallaron un poco cuando se echó a perder el aire acondicionado durante el verano, pero en general bien). Espero estar en su lista blanca por el resto de mi carrera científica.

1. INDEX

1.1. Contents

1.2. List of figures

1.3. Abbreviations

ACSF: Artificial cerebrospinal fluid

AMPAR: α-amino-3-hydroxy-5-methyl-4-isoxazolepropionic acid receptor.

CaM: Calmodulin.

CaMKII: Ca2+/calmodulin-dependent protein kinase II.

DIC: Differential interference contrast (microscopy)

EPSC: Excitatory postsynaptic current (evoked).

GABA$_A$ receptor: γ-aminobutyric acid type A receptor

HSP: Homeostatic synaptic plasticity.

KS: Kolmogorov-Smirnov.

LTD: Long-term depression.

LTP: Long-term potentiation.

mEPSC: Miniature excitatory postsynaptic current.

NMDAR: N-methyl-D-aspartate receptor.

PPF: Paired-pulse facilitation.

PSC: Postsynaptic current (evoked).

PTX: Picrotoxin.

SEM: Standard error of the mean.

TTX: Tetrodotoxin.

2. ABSTRACT

Homeostatic synaptic plasticity (HSP) is a diverse group of slow compensatory mechanisms allowing neurons to regulate their synaptic inputs according to network activity and is believed to contribute to the stabilization of Hebbian forms of synaptic plasticity (i.e., LTP, LTD). We previously described a form of HSP that develops between 5 to 13 hours after slicing rat hippocampus and is presumably triggered by the decrease in circuit activity due to deafferentation. To assess the mechanism of HSP, we investigated a possible role of CaMKII and its interaction with the glutamatergic NMDA receptor (NMDAR). CaMKII/NMDAR interaction has been extensively investigated in the context of LTP and may be a potential orchestrator of HSP. We show that after a pharmacological disassembly of this complex and transient inhibition of CaMKII, postsynaptic adaptations do not occur on time. Additionally, this form of HSP may be occurring in a context of altered hippocampal connectivity, as evoked excitatory postsynaptic current (EPSC) displayed polyphasic shapes, which may reflect the increased polysynaptic activity commonly observed in other models of neuronal deafferentation. In the presence of high concentrations of divalent cations used to isolate monophasic EPSC, we obtained preliminary evidence indicating that this HSP process preserves the AMPAR/NMDAR transmission and the GluN2B/GluN2A-NMDAR subunits ratio, indicating that this HSP process does not alter the information content of synapses. Finally, we tested whether this process involves the insertion of GluA1-homomeric AMPARs into synapses, which has been previously related

to some rapid forms of HSP. However, we did not found evidence supporting this possibility.

3. INTRODUCTION

Synaptic plasticity is the most widely studied candidate mechanism underlying learning and memory (Stuchlik, 2014; Takeuchi et al., 2014). One of the most well-known forms of synaptic plasticity is Hebbian plasticity, a group of correlation-based mechanisms that modify synapses in a specific manner, e.g. *long-term potentiation* (LTP) and *long-term depression* (LTD) (Bliss and Collingridge, 1993). However, Hebbian forms of plasticity may destabilize neuronal networks by an inherent positive feedback component (Miller and MacKay, 1994; for a review see Turrigiano, 2008). Conversely, other forms of synaptic plasticity, known as *homeostatic synaptic plasticity* (HSP), have been reported and proposed to counteract the destabilizing effects of Hebbian interactions, allowing neurons to maintain synaptic transmission within a physiologically suitable range that preserves network excitability (Turrigiano and Nelson, 2000, 2004; Turrigiano, 2008). In contrast to LTP and LTD, which can be induced in a short time scale (seconds), HSP forms are slow compensatory adaptations (mostly detected after several hours and up to days of altered excitability) that adjust cell excitability up or down, maintaining circuit stability (Turrigiano and Nelson, 2000, 2004; Turrigiano, 2008). HSP phenomena have been described in different contexts of altered excitability: after pharmacological blockade of action potentials or synaptic transmission in neuronal and organotypic cultures (O'Brien et al., 1998; Turrigiano et al., 1998; Kilman et al., 2002) and *in vivo* in the hippocampus (Echegoyen et al., 2007); in slices from primary visual and somatosensory cortices of light

1

deprived rats (Goel et al., 2006); and also in a context of deafferentation in organotypic hippocampal slices (Vlachos et al., 2012). Interestingly, we recently observed that a relatively fast form of HSP occurs few hours after fresh hippocampal slice preparation (Vergara, 2016).

HSP has usually been studied by measuring the miniature postsynaptic currents (minis) generated by the spontaneous release of neurotransmitter from unitary vesicles. Changes in minis amplitude suggest postsynaptic adjustments, whereas frequency variations are commonly interpreted as changes in the neurotransmitter release probability, implicating a presynaptic locus of HSP. Under some circumstances, HSP may involve a process of synaptic scaling, a cell-wide synaptic process in which each synapse scales up or down proportionally to its original synaptic weight (Turrigiano et al., 1998). Synaptic scaling may allow keeping synaptic transmission in a dynamics range without interfering with the relative strength of the synapses, preserving in this way the relative differences produced by previous LTP or LTD episodes. A process of synaptic scaling may be relevant to avoid the corruption of information in neural circuits, particularly in regions where Hebbian interactions are widely present, such as the hippocampus. HSP and synaptic scaling have been mainly reported in organotypic and cell cultures subjected to pharmacological manipulations (O'Brien et al., 1998; Turrigiano et al., 1998; Kilman et al., 2002). In contrast, the rapid HSP modification observed by us in hippocampal slices occurs in the absence of pharmacological manipulation and develops in the first 13 hours after

brain dissection. This homeostatic phenomenon is expressed as a rise in the frequency of mEPSC over time and a multiplicative scaling of their amplitudes and is presumably triggered by the decrease in circuit activity due to slicing (Vergara, 2016). This HSP form may be of particular interest to HSP phenomena, in particular, because it may take place in the first hours after stroke and other forms of traumatic brain injury. In this work, we studied the mechanism behind this HSP process.

3.1. A possible role of CaMKII and NMDAR in HSP.

Ca^{2+}/calmodulin-dependent kinase II (CaMKII) is a major component of glutamatergic synapses and has been related to both, Hebbian and homeostatic forms of synaptic plasticity (Lisman et al., 2002; Wang et al., 2011, 2013; Ranson et al., 2012; Shin et al., 2012). CaMKII, as a holoenzyme is formed of 6–12 subunits in variable ratios of the 52 kDa α isoform and the 60 kDa β isoform (Bennett et al., 1983). CaMKII may be a potential orchestrator of HSP, as α and β subunits are inversely regulated by neuronal activity in hippocampal cultures, defining their subcellular location and affinity for calcium, and thus their capability to interact with a diverse number of proteins at the postsynaptic densities (Thiagarajan et al., 2002). The intracellular location of CaMKII has a critical effect on synaptic transmission, as active CaMKII is translocated to synapses in an activity-dependent manner, increasing its enrichment in the postsynaptic density. CaMKII binds directly to the NMDAR, placing it in a suitable site to control synaptic strength (Shen and Meyer, 1999; Shen et al., 2000; Bayer et al., 2001; Lisman et

al., 2002). Moreover, this interaction may be a major factor in the maintenance of synaptic strength (Sanhueza et al., 2011), as synaptic depression is observed when the complex is disrupted but not when the activity of CaMKII is inhibited.

Given the evidence mentioned above, we studied the function of the CaMKII/NMDAR complex in the expression of HSP. To address the particular role of the CaMKII/NMDAR interaction on HSP, we pharmacologically disassembled the complex by using the CN21 peptide, a 21 amino-acid sequence derived from the CaMKIIN protein, which is a specific endogenous inhibitor of CaMKII (Chang et al., 1998; Vest et al., 2007). The CN21 peptide retains CaMKIIN specificity and inhibitory potency (Vest et al., 2007), which at 20 µM concentrations can disassemble CaMKII/NMDAR and has been previously used as a tool to study this interaction (Sanhueza et al., 2011; Barcomb et al., 2016). The CN21 peptide was fused to the cell-permeating peptide *tat* (Vivès et al., 1997), which allows CN21 to cross the plasmatic membrane.

3.2. Changes in neurotransmitter release probability: proposed mechanism for the increase in mEPSC frequency in acute slices.

The HSP process in hippocampal slices was expressed in part through a strong increase in the frequency of mEPSC (Vergara, 2016). This change may be due to presynaptic changes involving an increased neurotransmitter release probability. Other interpretations, such as the conversion of previously silent into functional synapses and an increase in the total number of synaptic contacts, are also possible. To address if this process is due to an increase in neurotransmitter

release probability, we evaluated changes in the paired-pulse facilitation (PPF) ratio with time (Branco and Staras, 2009). PPF is inversely related to the neurotransmitter release probability.

3.3. Does HSP preserve the metaplastic properties of synapses?

Metaplasticity makes reference to how susceptible are synapses to be modified (i.e. the plasticity of synaptic plasticity) (Abraham and Bear, 1996). The HSP process that we previously reported operates through a synaptic scaling mechanism of quantal amplitudes. This indicates that the HSP adaptations occurring after dissection in acute slices adjust the average transmission while preserving the relative differences between synapses weights. This might safeguard that HSP processes can normalize activity without fundamentally altering the relative information content of synapses. However, this information not only depends on the relative difference between synaptic weights but also on the metaplastic properties of the circuit. Interestingly, the properties of the synapses that mediate metaplasticity are preserved in many cases of HSP. For example, the proportion of NMDAR/AMPAR-mediated transmission and of GluN2B/GluN2A subunits of NMDARs are usually preserved in HSP (Umemiya et al., 1999; Gil and Amitai, 2000; Watt et al., 2000) and both may affect the threshold for LTP induction, and thus the metaplastic properties of synapses. Considering this, we examined whether the HSP adaptations occurring in acute slice also preserve the NMDAR/AMPAR transmission and GluN2B/GluN2A subunits ratio. The GluN2B/GluN2A subunits ratio defines the decay kinetics of

NMDAR-mediated currents, as receptors presenting the GluN2A subunit display faster-decaying kinetics than those presenting GluN2B subunit (Anantharam et al., 1992).

3.4. GluA1-homomeric AMPAR: a candidate for the rapid expression of HSP.

Although HSP phenomena were formerly observed after days of altered excitability (O'Brien et al., 1998; Turrigiano et al., 1998; Kilman et al., 2002), subsequent studies have reported relatively faster homeostatic adaptations occurring in a rapid temporal scale (~4 hours) (Sutton et al., 2006; Ibata et al., 2008; Vlachos et al., 2012), similarly as occurring in our model of HSP (Vergara, 2016).

NMDAR mediated transmission may be relevant in the temporal expression of some forms of HSP. In fact, its blockade, along with action potential inhibition, produces a rapid increase (~3 hours) in quantal amplitudes (Sutton et al., 2006). This particular case is mediated by local dendritic regulations and is mechanistically different to more typical slow forms of HSP (i.e. Turrigiano et al., 1998). Another interesting characteristic is that it occurs by a rapid surface expression of GluA1-homomeric AMPARs (or GluA2-lacking AMPAR) (Sutton et al., 2006; Wang et al., 2011), which presents increased inward rectification (a non-linear relation between channel current and membrane potential).

The reduced synaptic activity might be a key factor in our HSP model, since acute slices show smaller and less frequent mEPSC in comparison to cultures

(De Simoni et al., 2003; Szczot et al., 2010), which may mimic the effects of blocking NMDAR transmission in cultures. Taking this into account, it is possible that our HSP model operates through a similar mechanism. We addressed this possibility by measuring the amount of inward rectification of evoked excitatory postsynaptic currents (EPSC). EPSC rectification is associated with the proportion of GluA1-homomeric AMPARs.

4. HYPOTHESIS

The homeostatic adaptations occurring spontaneously in acute hippocampal slices require the CaMKII/NMDAR interaction for its proper expression, involve an increase in the neurotransmitter release probability, preserve the NMDAR/AMPAR transmission and GluN2B/GluN2A subunits ratio and are caused by the insertion of GluA1-homomeric AMPARs.

5. OBJECTIVES

General objective:

In relation to the HSP process in acute hippocampal slices:

To study the role of the CaMKII/NMDAR interaction in HSP in acute hippocampal slices and to evaluate possible changes in the neurotransmitter release probability, the NMDAR/AMPAR and GluN2B/GluN2A ratio and proportion of GluA1-homomeric AMPARs.

Specifics objective:

1. To evaluate mEPSC alterations with time after pharmacological disassemble of the NMDAR/CaMKII complex.
2. To evaluate changes in the neurotransmitter release probability with time.
3. To evaluate variations in the NMDAR/AMPAR dependent synaptic transmission and GluN2B/GluN2A subunits ratio with time.
4. To evaluate changes in the proportion of GluA1-homomeric AMPARs with time.

6. MATERIALS AND METHODS

6.1. Hippocampal slice preparations and animal treatments.

Animal care was in accordance to the institutional guidelines of the Bioethics Committee of the Faculty of Sciences, University of Chile. Transverse Hippocampal slices (350 µm) from 18- to 22-days old male Sprague-Dawley rats were prepared. For this, animals were anesthetized with diethyl ether and later decapitated. The brain was removed and placed in an ice-cold dissection solution containing (in mM): 125 NaCl, 2.6 KCl, 10 $MgCl_2$, 0.5 $CaCl_2$, 26 $NaHCO_3$, 1.23 NaH_2PO_4, and 10 D-glucose (equilibrated with 95% O_2 and 5% CO_2), pH 7.3. Slices were prepared using a vibratome (1000 plus, Vibratome®) and the CA3 area was removed. Subsequently, the slices were allowed to recover for a minimum of one hour at 30°C in an inverted interface chamber (tissue inserts, 8µm) maintained in an atmosphere saturated with 95% O_2 and 5% CO_2. Each insert held 2-3 slices submerged in a drop of 200 µL of artificial cerebrospinal fluid (ACSF) containing (in mM): 125 NaCl, 26 $NaHCO_3$, 1 NaH_2PO_4, 2.6 KCl, 2 $CaCl_2$, 1 $MgCl_2$, and 10 D-glucose. In experiments in which the slices were preincubated with the peptides, after one hour of recovering, the drop of solution bathing slices was carefully removed and replaced by freshly oxygenated ACSF containing 20 µM of tat-CN21 (test) peptide or scrambled control peptide (tat-SCR). Slices were incubated for 2 hours with these peptides, and then the solution was replaced by regular oxygenated ACSF and maintained for at least two hours before recordings. In experiments that did not involve peptides, regular

9

ACSF was used after recovering and maintained until the end of incubation (see 7.1 section).

6.2. Electrophysiological recordings.

For recordings, the slices were transferred to a submersion-type recording chamber mounted on an upright microscope (Nikon E600FN or Olympus BX51WI) equipped with differential interference contrast microscopy (DIC). The slices were continuously superfused (2–4 mL/min) with ACSF (same composition that in slice incubation) bubbled with 95% O2 and 5% CO_2. A total volume of 100 mL of ACSF was recirculated during each experiment using a two-way pump. The experiments were conducted at 30-31°C. Whole-cell patch-clamp recordings were performed with electrodes (2-5 MΩ) fabricated from borosilicate glass capillary tubing (0.8 - 1.10 x 100 mm; Kimble Glass Inc) using a horizontal puller (Flaming/Brown P- 97, Sutter Instrument Co). Voltage-clamp recordings were performed with an EPC-10 patch-clamp amplifier (Heka, Heidelberg, Germany); data were filtered with a 4-pole Bessel filter at 2.9 kHz and acquired at 20 kHz using the Heka PatchMaster software. All recordings were done in the presence of 100 µM picrotoxin (PTX; γ-aminobutyric acid type A receptor (GABA$_A$ receptor) blocker) except when otherwise specified and, in presences of 1 µM tetrodotoxin, for the mEPSC recordings, (TTX; voltage-dependent Na^+ channel blocker). Internal pipette solution was (in mL): 115 Cs methane sulfonate, 20 CsCl, 10 HEPES, 0.6 EGTA, 0.4 Na-GTP, 4 Na$_2$-ATP, 2.5 MgCl, and 10 Na$_2$-phosphocreatine, pH 7.25 (293 mOsm). Liquid junction potential was ~12 mV and was not corrected. mEPSC

were measured during 400 seconds at -60 mV. EPSC were evoked by stimulating the Schaffer-collateral pathway via a stimulation electrode placed at 100–200 µm from cell body layer. Stimulation intensity was adjusted to induce 50–150 pA EPSC at -70 mV. Series and input resistance were monitored throughout each experiment, and only those recording with a series resistance less than 31 MΩ (Vlachos et al., 2012). Cells with holding currents below -100 pA or input resistance above 90 MΩ were not considered in the analysis (typical input resistance of the recorded neurons is ~60 MΩ). A holding current below -100 pA is indicative of a depolarized resting potential, which is proper of CA1 interneurons (Rudy et al., 2011).

6.3.   Data analysis and statistical methods.

EPSC and mEPSC detection and analysis, and random permutation statistical analysis were done using a custom-built algorithm designed in IgorPro 6.03. Statistical tests were done with GraphPad Prism 7 and IgorPro 6.03. The requirement for the statistical test used (variance and normality of the samples) were assessed for each case using the Brown-Forsythe and the Shapiro-Wilk normality test, using an α value of 0.05.

7. RESULTS

7.1. Role of the CaMKII/NMDAR complex in the expression of HSP.

7.1.1. Experimental conditions.

We evaluated the role of the CaMKII/NMDAR interaction on HSP by measuring mEPSC after pharmacologically disassembling CaMKII/NMDAR complex using the tat-CN21 peptide. Because we are interested in studying this interaction without permanently inhibiting CaMKII, hippocampal slices were incubated with the tat-CN21 peptide for the time needed to disassemble the CaMKII/NMDAR complex (2 h), after which the peptide solution was washed away. Washing out the peptide potentially restores CaMKII activity but does not revert the CaMKII/NMDAR disassembling effect (Sanhueza et al., 2011; Barcomb et al., 2016). This method allowed us to study synaptic transmission after disassembling the CaMKII/NMDAR complex while kinase activity was potentially functional (Fig. 1).

HSP modifications were evaluated by recording cells in two intervals, 5 to 8 hours after slicing (T1) and 9 to 12 hours after slicing (T2). Time-dependent adaptations were evaluated in two different conditions: a test condition where slices were preincubated with the tat-CN21 peptide and a control condition where a scrambled version of tat-CN21 (tat-SCR, inactive version of tat-CN21) was used instead.
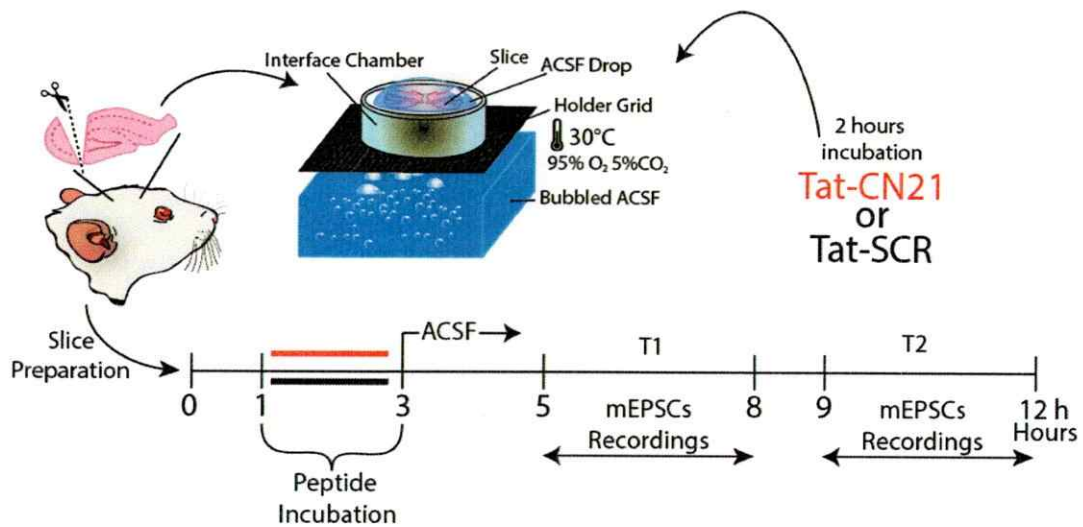
12

Figure 1. Experimental design used to evaluate CaMKII/NMDAR role on HSP. Hippocampal slices were prepared from 18-22 days old rats. CA3 area was removed, and slices were placed on an inverted interface chamber. Slices preparation denotes time 0. Slices were covered by a drop of ACSF, which after 1 hour of recuperation was gently replaced by another drop containing tat-SCR or tat-CN21 peptide in ACSF. Slices were incubated for two hours with these peptides, and then the covering solution was washout and replaced by freshly oxygenated ACSF. mEPSC recordings were done in two incubation time intervals; the first one 5 to 8 hours after slicing (T1) and the second one 9 to 12 hours after slicing (T2). Incubation and recordings were done at 30°C. See Material and Method for a detailed description.

7.1.2. *Discarding non-specific effects associated with tat-SCR (control) peptide treatment.*

First, we analyzed whether preincubation with tat-SCR peptide affects the HSP process that we previously reported (Vergara, 2016). Homeostatic adaptations taking place after slicing are expressed through a scaling up of quantal amplitudes and an increase in mEPSC frequency. Therefore, we would expect a similar dynamics with time for tat-SCR-pretreated slices. To evaluate this, we compared the mEPSC from neurons recorded in the T1 and T2 intervals in slices preincubated with the control peptide (Fig. 2). Fig. 2A shows a

representative current trace from each time interval. From these recordings, it is apparent an increase in mEPSC frequency and the appearance of a population of comparatively much larger events at later times. To evaluate if the amplitude, frequency or kinetics of the mEPSC are significantly different between the studied time intervals, we compared the average values of these parameters obtained for each cell recorded during the T1 and T2 intervals (Fig. 2B-E). Average amplitude (T1=9.33±0.34 pA, T2=12.27±0.35 pA, P <0.05) and frequency (T1=0.38±0.05 Hz, T2=2.43±0.51 Hz, P <0.0001) but not rise (T1=2.58±0.10 ms, T2=2.32±0.11 ms, P>0.05) or decay time (T1=7.24±0.65 ms, T2=6.75±0.26, P>0.05) were significantly different (Student t-test with Welch's correction for unequal variances, n=9 for T1 and T2) (Fig. 2). These results are in agreement with our previous observation (Vergara, 2016), suggesting that tat-SCR transient incubation does not affect the HSP process.
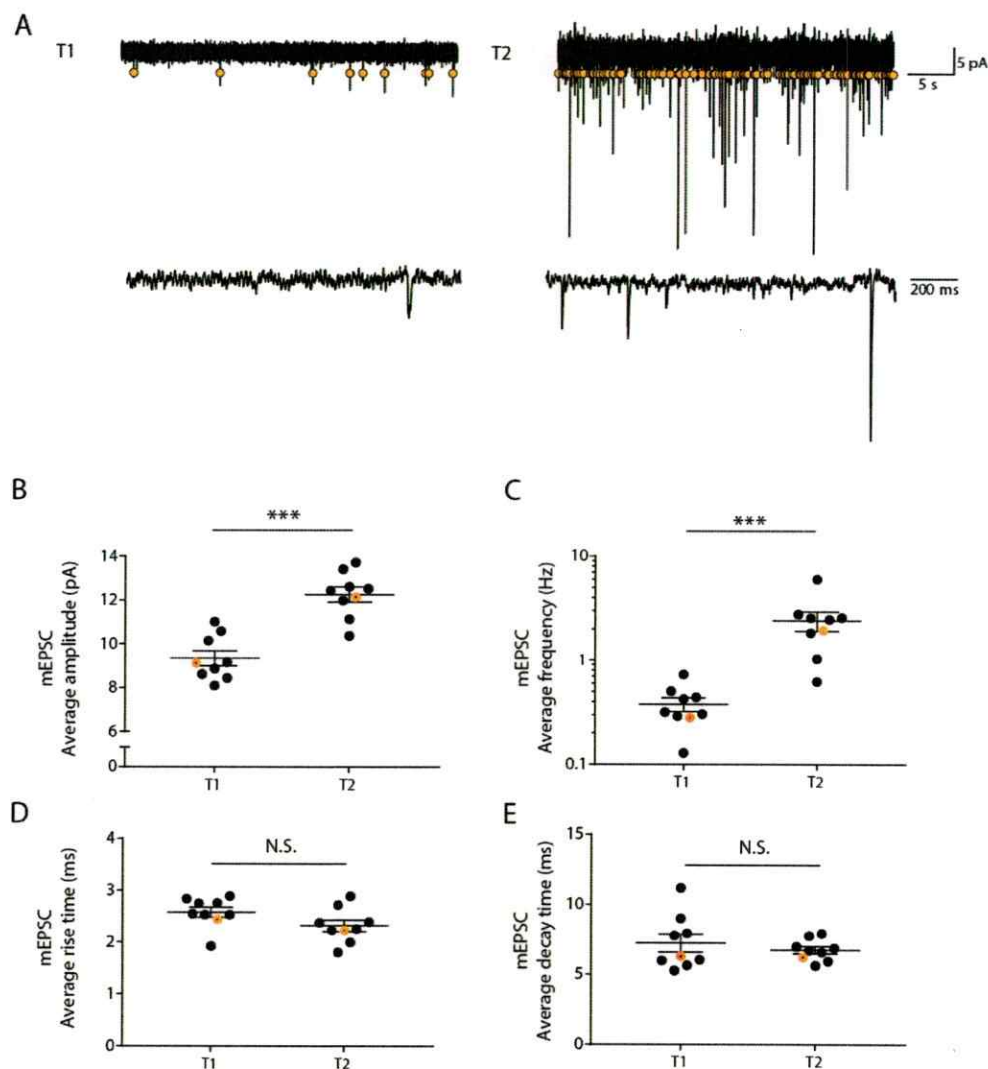
Figure 2. Effect of the tat-SCR peptide on HSP. (A) A representative recording from the T1 and T2 intervals. Two different time scales are shown for each condition. Yellow circles indicate detected events (B) Effect of time on mEPSC average amplitude in slice preincubated with the tat-SCR peptide. The hollow orange circles correspond to the recording shown in (A) (same for Figures C, D, and E). (C) Effect of time on mEPSC average frequency in slice preincubated with the tat-SCR peptide. Data were transformed to its log10 form. (D) Effect of time on mEPSC average rise time in slice preincubated with the tat-SCR peptide. (E) Effect of time on mEPSC average decay time in slice preincubated with the tat-SCR peptide. (*=P <0.05, ***=P <0.0001, Student t-test with Welch's correction for unequal variances. Horizontal bars denote mean and error bars standard error of the mean (SEM)).

Although the average mEPSC amplitudes increase with time, the question of how the distribution of events is changing requires further analysis. Our previous observations indicated that this HSP process operates through a multiplicative scaling-up rule. To test if tat-SCR pretreatment interferes with this dynamic, we compared the complete distribution of quantal amplitudes. Fig. 3A shows superimposed the cumulative probability plot of the amplitude distribution of each cell recorded during T1 and T2 intervals (gray and black curves, respectively). That plot suggests not only that the average amplitude increased with time, but that the entire distribution of mEPSC amplitudes shifted to the right, indicating a general tendency and further suggesting a HSP phenomenon. To evaluate whether the mEPSC amplitudes from the cells recorded during T1 and T2 interval are significantly different, we used a previously described random permutation statistical test (also known as Monte Carlo test) (Vergara, 2016). As expected, mEPSC amplitude distributions from both data samples are significantly different (random permutation test, $P=1\cdot10^{-4}$) (Fig. 3A), supporting that tat-SCR preincubation does not affect the ongoing HSP adaptations.

To test whether mEPSC amplitudes follow a scaling-up rule a commonly used approach was employed (Turrigiano et al., 1998). First, 45 events were randomly chosen from each cell and grouped into a single distribution used to represent the time intervals T1 and T2. Next, the events were rank ordered. To avoid outliers, data above 99% of the distribution was discarded (Kim and Alger, 2010; Sweatt, 2016). Finally, the distribution representing the interval T2 was plotted against the

distribution representing the interval T1 (Fig. 3B). If mEPSC amplitude increases through a synaptic scaling rule, then the relationship between the paired points must be well-represented by a linear function with slope larger than 1 (Turrigiano et al., 1998). Accordingly, paired data virtually overlapped with the linear fit $y=1.81 \cdot x-4.56$ ($r=0.99$), and if the T2 representing distribution is reverse-transformed using the parameters of the above linear equation, differences with the T1 representing distribution become not significant (two-sample Kolmogorov Smirnov (KS), $P=0.99$), validating the representation of the data by this fit. These results support a process of multiplicative synaptic scaling. However, it should be noted that we are describing the mEPSC amplitude relationship through a linear function that includes a multiplicative (the slope) and an additive factor (the y-axis intercept). A proportional increase in mEPSC amplitudes must not involve additive modifications, yet the intercept reflects those events that fall below the detection threshold (~5 pA) producing a wrong pairing of the distributions (Turrigiano et al., 1998; for a detailed description of this problem see Kim et al., 2012).

To discard the possibility of a HSP process involving additive modifications of quantal amplitudes, an alternative approach was additionally used (Kim et al., 2012; Soares et al., 2013; Vergara, 2016). If the mEPSC amplitude increases following a scaling-up rule, then a scaling factor must exist that, multiplying by it one distribution produces non-significant differences with the other. To evaluate this, we tested several scaling factors to determine the one producing the highest

P-value between interval I and III representing distributions (Fig. 3C). As we cannot create new events appearing above the detection threshold after upscaling, downscaling was performed instead, removing those events that fall below the detection threshold (defined as the smallest recorded mEPSC amplitude) (Kim et al., 2012) (Fig. 3C). A multiplicative factor of 1.43 was determined as the best possible scaling factor, as it yielded the highest P-value in the comparison between the amplitude distributions representing T1 interval and the downscaled amplitude distribution representing T2 interval (two-sample KS, P=0.31) (Fig. 3D).

Finally, we tested whether this scaling factor produces statistically indistinguishable sets of curves, considering the complete distribution of events in each cell instead of a small fixed random sample (Fig. 3E). When the events from each cell recorded during the T2 interval were downscaled by this factor, the corresponding cumulative probability plots were not significantly different to the plots from the T1 interval (random permutation test, P=0.25). This dynamics is consistent with a process of multiplicative synaptic scaling of quantal amplitudes, and hence to our previous observations in untreated slices (Vergara, 2016), corroborating that preincubation with tat-SCR peptide does not have any effect on HSP.
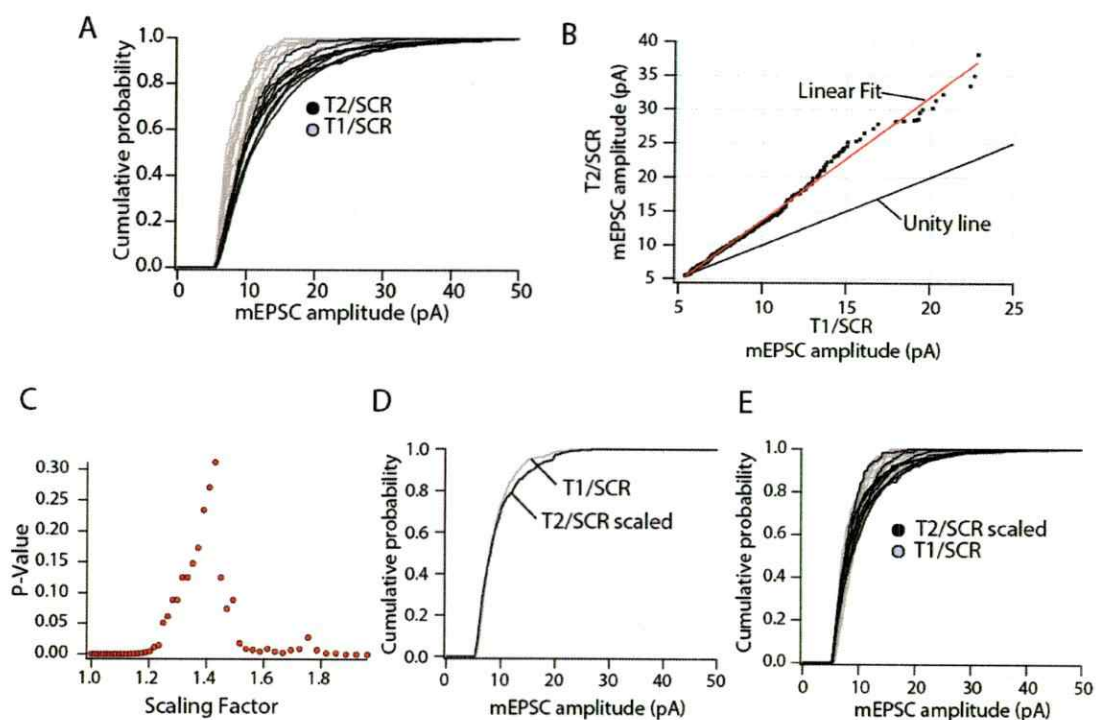
Figure 3. mEPSC amplitude from slices incubated with the control peptide increases in time following a scaling-up rule. (A) Cumulative probability plot of the mEPSC amplitude distribution of each cell recorded in the T1 (gray) and T2 (black) intervals. (B) A representing distribution for T2 interval was created by grouping 45 randomly selected events from each cell. Resulting distribution was plotted against its equivalent from the T1 interval (black points). Red line is a linear fit described by the equation y=1.81·x-4.56 (r=0.99). Unity line is a linear function with slope=1 representing the expected plot for two equal distributions. (C) Different scaling factors were tested to obtain the one producing the highest P-value after downscaling the distribution representing T2 interval and comparing it with the one for T1 interval through a two-sample KS (the best scaling factor obtained is 1.43). (D) Cumulative probability plot of the representing distribution for a T2 interval after being downscaled by the factor 1.43 plotted superimposed with the representing distribution for the T1 interval. (E) Cumulative probability plots of the mEPSC amplitude distribution of each cell recorded during T1 (gray) and of each cell recorded during T2 after being downscaled by the factor 1.43 (black).

7.1.3. Tat-CN21 preincubation effect on HSP.

Having confirmed that the tat-SCR peptide does not alter HSP, we compared the

mEPSC amplitude distribution from neurons recorded during the T1 and T2

intervals in slices preincubated with the tat-CN21 peptide (Fig. 4). Fig. 4A shows a representative current trace from each interval. An increase in mEPSC frequency is evident in the T2 recording, but, and in contrast to control peptide treatment, a rise in amplitude is not evident, suggesting that a postsynaptic locus of HSP is not expressed after tat-CN21 preincubation. Accordingly, only the average frequency (T1=0.54±0.12 Hz, T2=2.69±0.26 Hz, P<0.0001), but not the average amplitude (T1=11.01±0.40 pA, T2=10.56±0.33 pA, P>0.05) or kinetics (rise: T1=2.35±0.10 ms, T2=2.37±0.09 ms, P>0.05. Decay: T1=6.33±0.40 ms, T2=6.59±0.42 ms, P>0.05) were significantly different between groups (Student t-test with Welch's correction for unequal variances). Accordingly, when we compared the cumulative probability plot of the amplitude distribution of each cell recorded during T1 and T2 intervals (Fig. 5, light red and bold red curves, respectively), plots virtually overlapped and the differences between data sets were not significant (random permutation test; P=0.875). These results indicate that the postsynaptic HSP adaptations previously reported do not occur after tat-CN21 preincubation, which is related to the transient inactivation of CaMKII and the disassembly of the NMDAR/CaMKII complex.
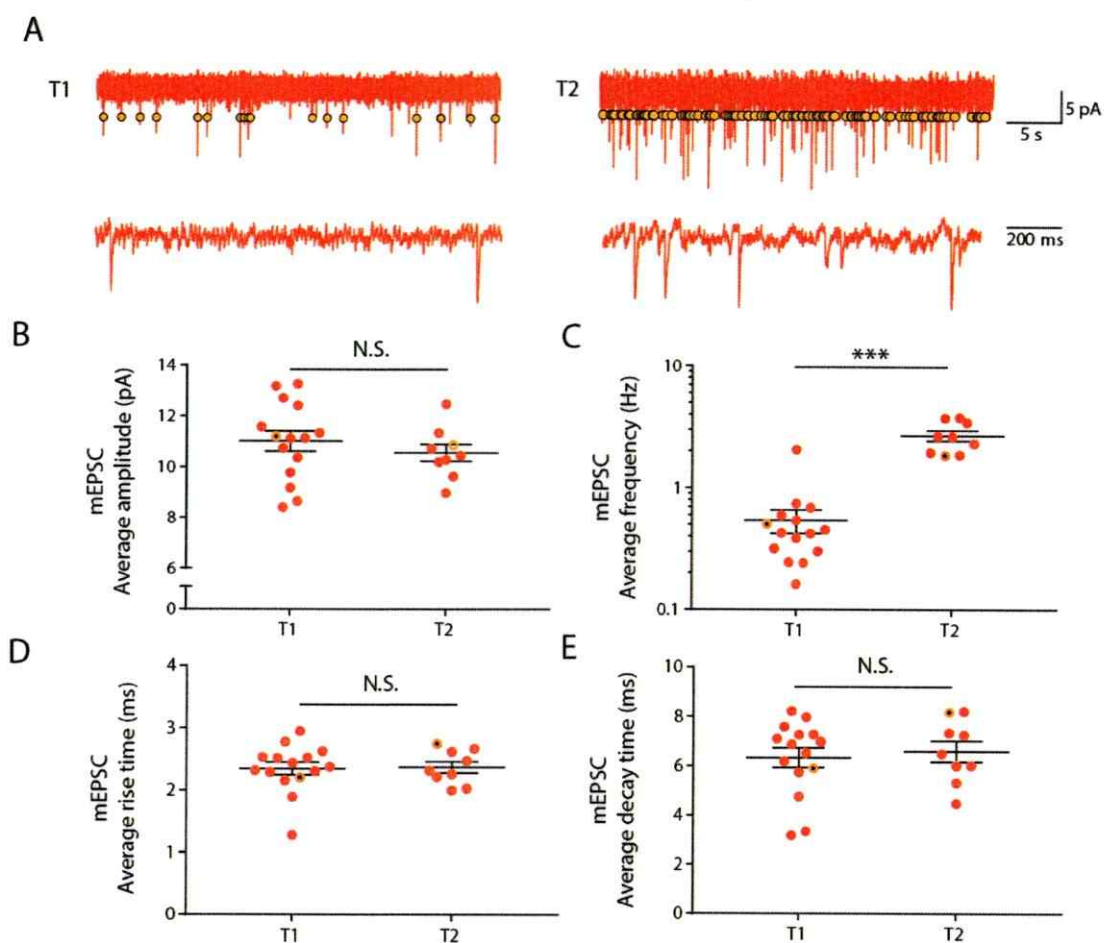
Figure 4. Effect of tat-CN21 peptide preincubation on HSP. (A) Representative recording at T1 and T2. Two different time scales are shown for each condition. (B) Effect of time on mEPSC average amplitude in cells from slices preincubated with the tat-CN21 peptide. The hollow orange circles correspond to the recording shown in (A) (same for Figures C, D, and E). (C) Effect of time on mEPSC average frequency in slice preincubated with the tat-CN21 peptide. Data were transformed to its log10 form. (D) Effect of time on mEPSC average rise time in slice preincubated with the tat-CN21 peptide. (E) Effect of time on mEPSC average decay time in slice preincubated with the tat-CN21 peptide. (***=P <0.0001, Student t-test with Welch's correction for unequal variances. Horizontal bars denote mean and its SEM, n =15 and 9 for T1 and T2, respectively).

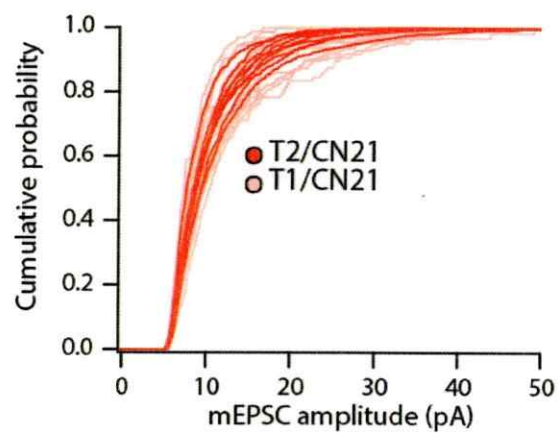**Figure 5.** **No amplitude increase of mEPSC occurs after transient incubation with the tat-CN21 peptide.** Cumulative probability plots of the mEPSC amplitude distribution of each cell recorded during T1 (light red) and T2 (bold red).

7.2. Analysis of evoked EPSC.

7.2.1. *Setting up of experimental conditions.*

We performed whole-cell patch clamp recording to measure evoked postsynaptic currents (PSCs) in neurons from the CA1 pyramidal layer. For the analysis of PSCs, two groups of cells were recorded: on group 5 to 8 hours post-slicing (T1) and another 9 to 12 hours post-slicing (T2). Experimental conditions were the same as mentioned in section 7.1 (Fig. 1), but without peptide treatment.

First, to determine the optimal experimental conditions, we evaluated the average evoked current obtained at different holding potentials for one cell recorded during the T1 interval (Fig. 6). The reversal potential of the evoked current (~-28 mV) was different from zero, indicating that this response is not exclusively glutamatergic. This non-zero reversal potential can be due to the recruitment of inhibitory inputs along with Shaffer collaterals. To test this possibility, we evaluated the evoked responses after the perfusion of the $GABA_A$ receptor antagonist picrotoxin (PTX) (Fig. 7A). Evoked response at +40 mV and -70 mV were drastically reduced after PTX bath application (Fig. 7B), indicating that the evoked response previously recorded were primarily GABAergic.
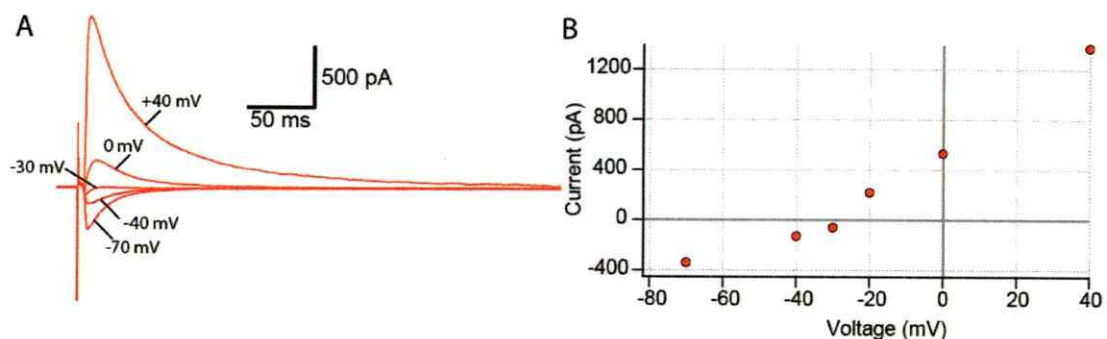
Figure 6. The reversal potential of the evoked currents is different from zero. (A) Average response of 10 evoked PSC at increasing holding potential from one cell recorded during the T1 interval. (B) The peaks of the traces shown in (A) were plotted against their respective holding potential. The reversal potential of the evoked response is ~-28 mV.
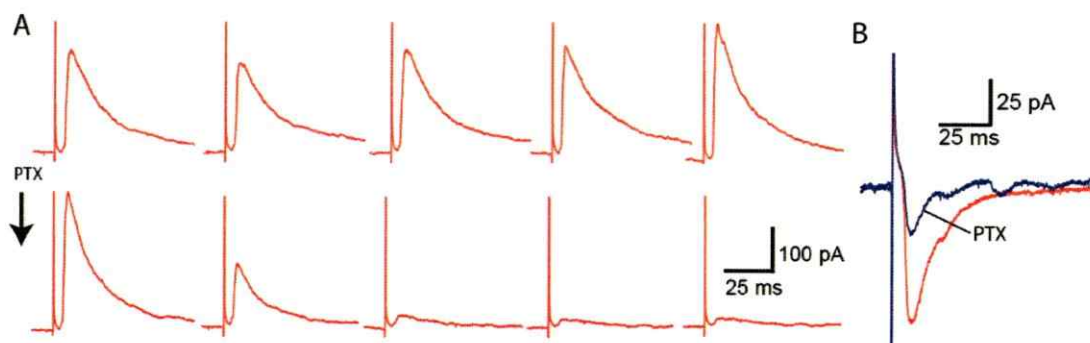

Figure 7. Isolation of EPSC after bath application of PTX. (A) Ten consecutive evoked PSC at +40 mV holding potential. The interval between stimulations was 25 seconds. After five consecutive PSCs, PTX was added to the bath (indicated by a black arrow). Evoked responses after PTX application are drastically reduced in the following 75 seconds. (B) Evoked response at -70 mV before and after PTX treatment (red and blue trace respectively).

However, although excitatory postsynaptic currents (EPSCs) were isolated in the presence of PTX, evoked responses displayed an irregular shape when compared with EPSCs from slices incubated in submersion chambers (Fig. 8A). This complex dynamics probably reflects a polysynaptic response caused by the sprouting of recurrent axons as a consequence of axonal deafferentation, a

process that has been reported to occur following axonal lesions in the cortex (Mckinney et al., 1997). Moreover, polysynaptic responses have been reported in some cases in the CA1 region of rat hippocampal slices after PTX treatment (Crépel et al., 1997). Another possible explanation is that this complex profile reflects asynchronous neurotransmitter release (Kaeser and Regehr, 2014).
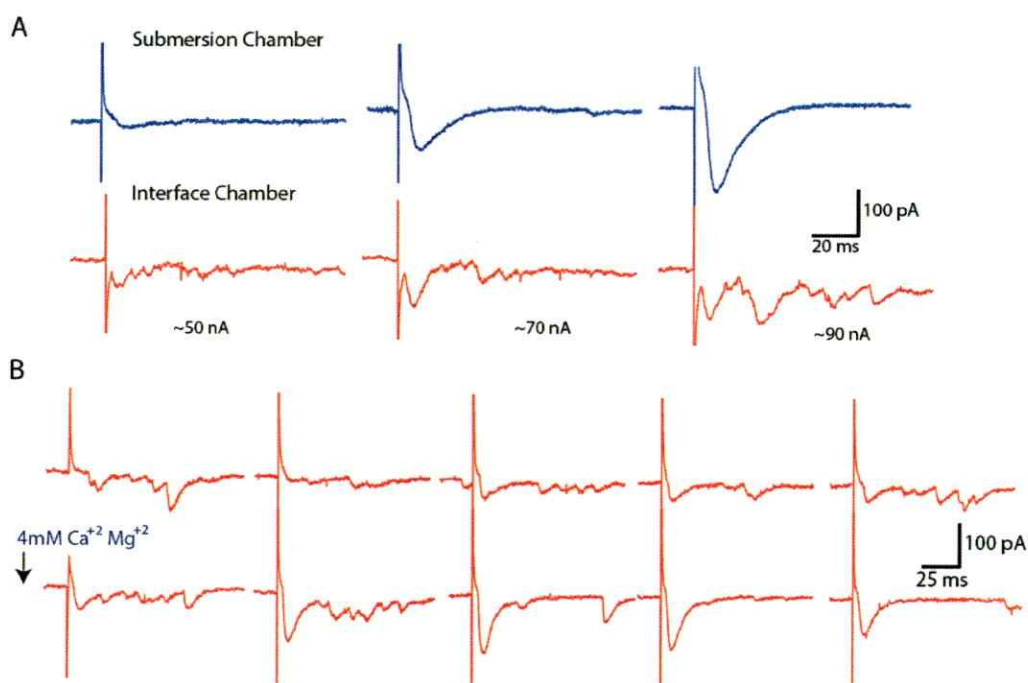
Figure 8. Irregular shapes of EPSC from slices incubated in interface chambers. (A) Representative evoked responses to different stimulation intensities in neurons from slices incubated in a submersion chamber (blue traces) or interface chamber (red traces). Evoked responses in neurons from interface chamber-incubated slices display a complex profile. (B) Ten consecutive evoked EPSC. The interval between stimulations was 25 seconds. After five consecutive EPSC, Ca^{2+} and Mg^{2+} was added to the bath up to a final concentration of 4mM (indicated by a black arrow). Evoked response in the following two minutes displayed a monophasic profile.

The complex profile of the evoked EPSCs makes analysis unfeasible. To deal with this issue, we evaluated evoked responses under high divalent concentration

(4 mM Ca^{2+} and Mg^{2+}), a strategy that has been previously used to isolate a monophasic response (Crépel et al., 1997; Liao and Walters, 2002; Sivaramakrishnan et al., 2013). Increases in the concentration of divalent cations raise the firing threshold by enhancing the surface charge (Hille et al., 1975), which is thought to prevent polysynaptic inputs from reaching firing threshold (Sivaramakrishnan et al., 2013). Accordingly, when the concentration of divalent cations in the bath was raised to 4 mM, the polyphasic responses were abolished (Fig. 8B). In light of this, an extracellular solution containing 4 mM of Ca^{2+} and Mg^{2+} was used to record EPSCs (only during recording but no during incubation, most of the time slices were kept in normal Ca^{2+} and Mg^{2+} concentrations). However, it is crucial to emphasize that this condition will not be entirely comparable to our previous results (Vergara, 2016), as an increase in extracellular calcium and magnesium may have a substantial effect on our measurements, even if it is only modified during the recordings. Therefore, the following results must be considered only as preliminary and by no means conclusive.

7.2.2. *Paired Pulse facilitation analysis.*

Previous results revealed a significant increase in mEPSC frequency (Vergara, 2016). This could be explained by a presynaptic locus of HSP involving changes in neurotransmitter release probability. To evaluate this, we compared the paired-pulse facilitation (PPF) ratio of the group of cell recorded during T1 and the group of cell from T2 intervals (Branco and Staras, 2009). Schaffer collaterals were

consecutively stimulated with a 50 ms interval, and PPF was estimated as the quotient between the peak amplitude of the second and the first EPSC (Fig. 9). No significant differences were found between T1 and T2 groups (Median PPF: T1=2.045; T2=2.025. Mann-Whitney test, P=0.89). Thus, no evidence supporting modifications in the probability of neurotransmitter release was obtained in the current conditions.
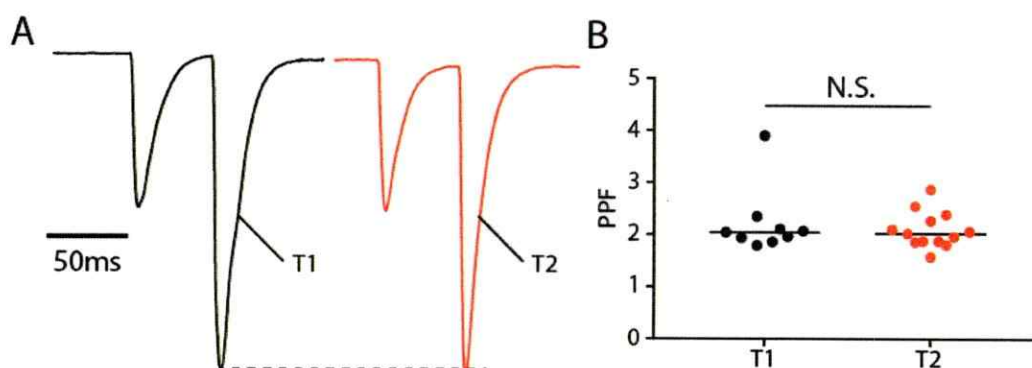

Figure 9. No evidence supporting that HSP involves changes in neurotransmitter release probability was found. (A) Average PPF current trace of the cells recorded at T1 and T2. Current traces are normalized relative to the peak of the first evoked current. The response in each cell was calculated by averaging ten repetitions. (B) Paired-pulse facilitation of each of the cells recorded during T1 and T2 intervals (N.S: P=0.89, Mann-Whitney test. Horizontal lines denote median. N=9 and 13 for T1 and T2, respectively).

7.2.3. *Analysis of the NMDAR decay time and the NMDAR/AMPAR transmission ratio.*

Under some circumstances, HSP may regulate average transmission without interfering with the information content of synapses. This depends on synaptic scaling but also on the metaplasticity properties of synapses (i.e., changes in the

susceptibility of synapses to undergo plastic modifications). Metaplasticity is related to NMDAR transmission and NMDAR subunit composition (Abraham and Bear, 1996; Yashiro and Philpot, 2008). We addressed whether the HSP form that we described also preserves NMDAR subunit composition and NMDAR/AMPAR ratio. To evaluate modifications in the proportion of GluN2A and GluN2B subunits, we measured the decay time constant of the evoked responses at +40 mV (Fig. 10). As previously described, NMDAR decay time constant was estimated by fitting a double exponential function (Anantharam et al., 1992). No changes in NMDA kinetics were observed between the different post-slicing intervals (median NMDAR decay τ: T1=109.8 ms; T2=113.3 ms. Mann-Whitney test, P=0.744), which suggests that NMDAR subunit proportion is preserved in HSP.

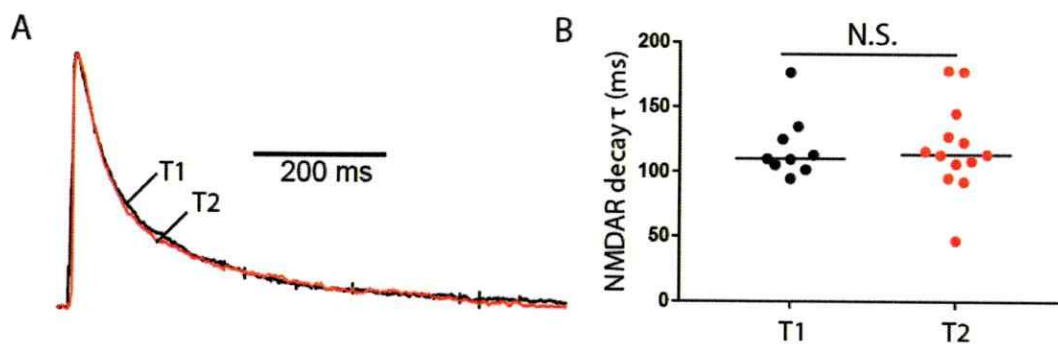
Figure 10. HSP would not involve changes in NMDAR subunit composition. (A) Average normalized EPSC of the cells recorded at T1 and T2. The response in each cell was calculated by averaging ten repetitions. (B) NMDAR decay τ of the cells recorded during the T1 and the T2 intervals. (N.S: P=0.744, Mann-Whitney test. Horizontal lines denote median. N=9 and 13 for T1 and T2, respectively.

Next, we evaluated whether AMPAR and NMDAR-mediated transmission are scaled proportionally. To explore possible changes in the proportion of NMDAR and AMPAR constituents of the evoked EPSCs, we measured the ratio between the late component of the evoked response at +40 mV and the peak of the evoked response at -70 mV (Fig. 11). No differences were seen in the NMDAR/AMPAR ratio (median NMDAR/AMPAR ratio: T1=0.293; T2=0.254. Mann-Whitney test, P=0.39), suggesting that if AMPARs and NMDARs are being inserted into synapses, they do it in a similar proportion.

Figure 11. HSP would not involve changes in NMDAR/AMPAR transmission ratio. (A) Average evoked response at -70 and 40 mV from the cells recorded in the T1 and T2 intervals. Current traces were normalized relative to the peak of the evoked current at -70 mV. NMDAR/AMPAR ratio was calculated by measuring the ratio between the late component of the evoked response at +40 mV (80 ms after the stimulus artifact, denoted by arrows) and the peak of the evoked response at -70 mV. The response in each cell was calculated by averaging ten

repetitions. (B) NMDAR/AMPAR ratio of the recorded cells. (N.S: P=0.39, Mann-Whitney test. Horizontal lines denote median. N=9 and 13 for T1 and T2, respectively).

7.2.4. *Analysis of the EPSC rectification.*

Some forms of fast HSP involve the insertion of AMPARs carrying GluA1 homomers (Sutton et al., 2006). Given that GluA1 homomers increase inward rectification of AMPARs, we evaluated this possibility by estimating the magnitude of rectification in the cells recorded during the T1 and T2 intervals. Rectification was estimated as the ratio between the peak of the EPSC at -70 and +40 mV (Fig. 12). No significant difference in the magnitude of rectification was observed (Median rectification: T1=1.607, T2=1.502. Mann-Whitney test, P=0.948). Suggesting that the proportion of GluA1 homomers is preserved in these conditions.

It is important to mention that we are evaluating AMPAR rectification without blocking the NMDAR component of transmission at +40 mV. However, our results indicate that the NMDAR/AMPAR ratio is not modified either, meaning that any modification in the early component of the evoked response at +40 mV will reflect the AMPAR component of transmission.

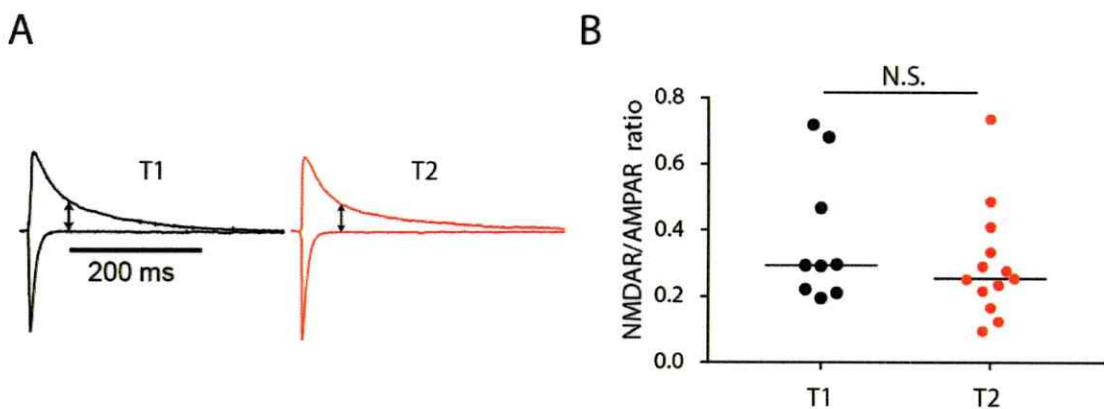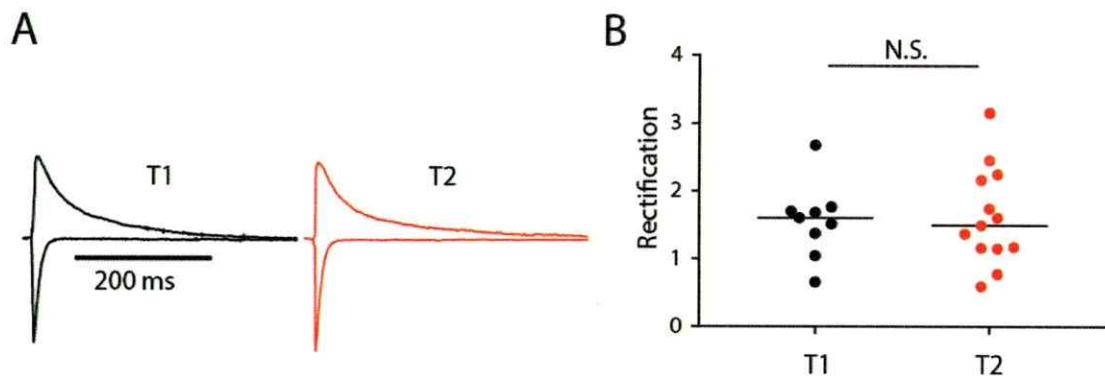**Figure 12. HSP would not involve changes in EPSC rectification.** (A) Average evoked response at -70 and 40 mV from cells recorded during T1 and T2 intervals. Current traces were normalized relative to the peak of the evoked current at -70 mV. The response in each cell was calculated by averaging ten repetitions. (B) Rectification of the cells recorded during T1 and T2 intervals (N.S: P=0.948, Mann-Whitney test. Horizontal lines denote median. N=9 and 13 for T1 and T2, respectively).

8. DISCUSSION

In this work we studied the mechanisms behind the HSP adaptations occurring without pharmacological manipulation in acute hippocampal slices. We studied the role of CaMKII and its interaction with the NMDAR receptor in this process, given that CaMKII/NMDAR complex may be a potential sensor of activity and orchestrator of synaptic function. Additionally, we also studied whether the increase in mEPSC frequency occurring with time is due to an increase in neurotransmitter release probability. Additionally, the preservation of the metaplastic properties of synapses in this HSP process was studied as changes in AMPA/NMDAR ratio and NMDAR kinetics. Finally, we evaluated if the postsynaptic modifications that we previously reported occur through the insertion of homomeric-GluA1 AMPARs.

8.1.   Role of the CaMKII/NMDAR complex in the expression of HSP.

We studied the role of CaMKII/NMDAR interaction in our model of HSP using the CaMKIIN-derived peptide tat-CN21 and tat-SCR. First, we corroborate that tat-SCR peptide has no unspecific effect on HSP (e.g. by an indirect effect of the tat sequence), and therefore can be used as a control condition. This is important because, for instance, other cell permeating proteins like ant/penetratin compromise CaMKII-selectivity by direct binding to CaM (Buard et al., 2010).

32

8.1.1. _Tat-SCR peptide (control) treatment has no incidental effect on HSP_

Our results indicate there is no effect of peptide treatment on HSP, since transient incubation with tat-SCR peptide did not affect the homeostatic adaptations that we previously observed (Vergara, 2016). Accordingly, when comparing the mEPSC from the cells recorded during the T1 and T2 intervals, mEPSC amplitude and frequency rose with time, and their amplitude increase was in agreement with a synaptic scaling dynamics.

8.1.2. _Tat-CN21 effect on HSP._

Our data indicate that transient incubation with tat-CN21 prevents the synaptic adaptations occurring with time, at least in the time interval studied. We conclude this because the average amplitudes and the cumulative probability plots of the mEPSC amplitude distribution from the cells recorded during the T1 interval were no significantly different to their equivalent at T2. Given that tat-CN21 treatment disassembles the CaMKII/NMDAR complex, one possible interpretation is that CaMKII/NMDAR interaction is necessary for the proper expression of HSP. This is consistent with the possibility that CaMKII/NMDAR may act as a synaptic strength orchestrator. However, it could also be that the synaptic adaptation occurring in time were prevented by a transient inhibition of the CaMKII kinase activity. One potential experiment to distinguish between these two possibilities may be to incubate slices with a lower peptide concentration (i.e. 5 µM), which is

33

enough to inhibit CaMKII activity but does not interfere with the CaMKII/NMDAR complex (Sanhueza et al., 2011).

Previous works have associated two effects for tat-CN21 peptide over synaptic transmission; one associated with the inhibition of CaMKII and another associated to the disassembly of the CaMKII/NMDAR complex (Sanhueza et al., 2011). Interestingly, the evidence suggests that CaMKII inhibition effect does not persist in time after washing the peptide, while the effect related to CaMKII/NMDAR disassembly endures for at least three hours (and probably more) (Sanhueza et al., 2011; Barcomb et al., 2016). This means that at least at the beginning of T1 interval the CaMKII catalytic activity is functional, but the CaMKII/NMDAR complex has not been reassembled, which argues in favor of the hypothesis that it is the CaMKII/NMDAR complex disassembly what prevents the expression of the postsynaptic locus of HSP.

Overall, our data demonstrate that after tat-CN21 transient incubation, which is related to the disruption of the CaMKII/NMDAR complex and transient CaMKII inhibition, the postsynaptic expression of HSP does not occur.

8.2. Evoked EPSC.

Stimulation of the Shaffer collaterals produced evoked currents with complex profiles (evoked currents with polyphasic shape, see section 7.2.1). Considering the deafferentation context, this probably results from polysynaptic activity. However, this could also be caused by events induced by asynchronous release

of neurotransmitter. To obtain a monophasic EPSC, we increased the extracellular concertation of divalent cations, an approach that is commonly used to isolate the monosynaptic components from polysynaptic evoked currents (Crépel et al., 1997; Liao and Walters, 2002; Sivaramakrishnan et al., 2013). Polysynaptic activity is a reasonable possibility, considering our experimental conditions it is feasible that axonal lesions during slice preparation induced a process of axonal sprouting, which may increase recurrent activity in the CA1 layer of the hippocampus (Deller and Frotscher, 1997; Mckinney et al., 1997; Verbich et al., 2016), leading to polysynaptic activity (Mckinney et al., 1997). Importantly, recurrent activity exists in the CA1 layer of the hippocampus, although not as prominent as in the CA3 layer (Crépel et al., 1997). CA1 recurrent activity may be enhanced in our experimental conditions. These results suggest that the modifications occurring in our HSP model are similar to those usually observed after deafferentation *in vivo* and *in vitro* (Deller and Frotscher, 1997; Vlachos et al., 2012), where polysynaptic activity is usual. Moreover, these results further validate our HSP model as a potential tool to study deafferentation-induced synaptic plasticity, since it integrates many of the phenotypes following neural lesions *in vivo* (Deller and Frotscher, 1997).

To address the questions proposed in this work and to make the analysis feasible, we used a higher concentration of divalent cations during the recordings. However, this approach has its drawbacks, because it makes our results less comparable with our previous observations (Vergara, 2016). Still, this

approximation may be useful as a preliminary approach to evaluate potential modifications occurring with time.

Previously, we reported that mEPSC frequency increase with time after slicing (Vergara, 2016), which may be explained by an increase in the probability of neurotransmitter release. However, we did not observe changes in the PPF ratio. This discrepancy may be due to the high divalent cation concentration used, which may hinder ongoing presynaptic homeostatic modifications. In particular, divalent cation concentrations can importantly affect neurotransmitter release probability (Bennett et al., 1989). Thus, we cannot rule out that this HSP process involves changes in neurotransmitter release probability.

We also wondered whether this HSP process alters the metaplastic properties of the circuit. The NMDAR subunit composition and the proportion of NMDAR- and AMPAR-mediated transmission can importantly affect metaplasticity (Abraham and Bear, 1996; Yashiro and Philpot, 2008). We evaluated if these two properties are being modified in this HSP process. Changes in NDMAR subunit composition were addressed by measuring the decaying time of the evoked response at +40 mV (which is related to NMDAR subunit composition, see above). We did not observe significant variations in any of these two parameters with time. This is in agreement with previous reports, as neither NMDAR decaying time or NMDAR/AMPAR transmission ratio is usually modified in other HSP models (Umemiya et al., 1999; Gil and Amitai, 2000; Watt et al., 2000). Overall, these results are consistent with the idea that HSP preserves the information content of

the synapses. However, further approaches are required to corroborate these observations, given that we have altered the divalent cation extracellular concentrations during recordings.

Finally, we determined whether the rise in mEPSC amplitude that we previously reported is occurring through the insertion of GluA1-homomeric AMPARs, which is related to the expression of some rapid forms of HSP (Sutton et al., 2006). We addressed this possibility by evaluating changes in the amount of rectification of EPSCs (GluA1-homomeric AMPARs are inward rectifiers, see above). Our results indicate that the magnitude of EPSC rectification is preserved in time, suggesting that this HSP form probably operates through a different mechanism. In agreement, other mechanisms for rapid HSP have been reported. For example, a fast scaling of quantal amplitudes that does not involve an increase in the proportion of AMPARs carrying GluA1 homomers has been described in optimized culture conditions, for example, including a bed of glia below neurons (Ibata et al., 2008). To further validate these results, we are also evaluating possible changes in the proportion of AMPARs subunits using immunoblotting techniques.

Overall, although our observations regarding NMDAR kinetics, NMDAR/AMPAR ratio and EPSC rectification are only suggestive, results are consistent with previous reports. In the case of PPF, variations with time may have been obscured by the increased divalent cation concentration. Additionally, we can conclude that the HSP process occurring in acute hippocampal slices takes

place in a context of altered synaptic function given the complex profile of the EPSC observed with a low concentration of divalent cations.

9. CONCLUSIONS

The postsynaptic homeostatic adaptations do not occur in slices preincubated with tat-CN21 peptide, and thus, after CaMKII transient inhibition and the disassembly of the CaMKII/NMDAR complex.

In a context of high divalent cations concentration during recording, no changes in the probability of neurotransmitter release, NMDAR decaying kinetics, NMDAR/AMPAR transmission ratio, or glutamatergic rectification are observed within the first 12 hours after hippocampus slicing

10. REFERENCES

Abraham WC, Bear MF. 1996. Metaplasticity: The plasticity of synaptic plasticity. Trends Neurosci 19:126–130.

Anantharam V, Panchal RG, Wilson A, Kolchine V V., Treistman SN, Bayley H. 1992. Combinatorial RNA splicing alters the surface charge on the NMDA receptor. FEBS Lett 305:27–30.

Barcomb K, Hell JW, Benke TA, Bayer KU. 2016. The CaMKII/GluN2B protein interaction maintains synaptic strength. J Biol Chem 291:16082–16089.

Bayer KU, De Koninck P, Leonard AS, Hell JW, Schulman H. 2001. Interaction with the NMDA receptor locks CaMKII in an active conformation. Nature 411:801–805.

Bennett M, Erondu N, Kennedy M. 1983. Purification and characterization of a calmodulin-dependent protein kinase that is highly concentrated in brain. J Biol Chem 2:12735–12744.

Bennett MR, Lavidis NA, Lavidis-Armson F. 1989. The probability of quantal secretion at release sites of different length in toad (Bufo marinus) muscle. J Physiol 418:235–249.

Bliss T V, Collingridge GL. 1993. A synaptic model of memory: long-term potentiation in the hippocampus. Nature 361:31–39.

Branco T, Staras K. 2009. The probability of neurotransmitter release: variability and feedback control at single synapses. Nat Rev Neurosci 10:373–83.

Buard I, Coultrap SJ, Freund RK, Lee Y-S, Dell'Acqua ML, Silva AJ, Bayer KU. 2010. CaMKII "Autonomy" Is Required for Initiating But Not for Maintaining Neuronal Long-Term Information Storage. J Neurosci 30:8214–8220.

Chang BH, Mukherji S, Soderling TR. 1998. Characterization of a calmodulin kinase II inhibitor protein in brain. Neurobiology 95:10890–10895.

Crépel V, Khazipov R, Ben-Ari Y. 1997. Blocking GABA(A) inhibition reveals AMPA- and NMDA-receptor-mediated polysynaptic responses in the CA1 region of the rat hippocampus. J Neurophysiol 77:2071–82.

Deller T, Frotscher M. 1997. Lesion-induced plasticity of central neurons: Sprouting of single fibres in the rat hippocampus after unilateral entorhinal cortex lesion. Prog Neurobiol 53:687–727.

De Simoni A, Griesinger CB, Edwards FA. 2003. Development of rat CA1 neurones in acute versus organotypic slices: role of experience in synaptic morphology and activity. J Physiol 550:135–47.

Echegoyen J, Neu A, Graber KD, Soltesz I. 2007. Homeostatic plasticity studies using in vivo hippocampal activity-blockade: Synaptic scaling, intrinsic plasticity and age-dependence. PLoS One 2.

Gil Z, Amitai Y. 2000. Evidence for proportional synaptic scaling in neocortex of intact animals. Neuroreport 11:4027–4031.

Goel A, Jiang B, Xu LW, Song L, Kirkwood A, Lee H-K. 2006. Cross-modal regulation of synaptic AMPA receptors in primary sensory cortices by visual experience. Nat Neurosci 9:1001–3.

Hille B, Woodhull AM, Shapiro BI. 1975. Negative surface charge near sodium channels of nerve: divalent ions, monovalent ions, and pH. Philos Trans R Soc Lond B Biol Sci 270:301–18.

Ibata K, Sun Q, Turrigiano GG. 2008. Rapid Synaptic Scaling Induced by Changes in Postsynaptic Firing. Neuron 57:819–826.

Kaeser PS, Regehr WG. 2014. Molecular Mechanisms for Synchronous, Asynchronous, and Spontaneous Neurotransmitter Release. Annu Rev Physiol 76:333–363.

Kilman V, van Rossum MCW, Turrigiano GG. 2002. Activity deprivation reduces miniature IPSC amplitude by decreasing the number of postsynaptic GABA(A) receptors clustered at neocortical synapses. J Neurosci 22:1328–1337.

Kim J, Alger BE. 2010. Reduction in endocannabinoid tone is a homeostatic mechanism for specific inhibitory synapses. Nat Neurosci 13:592–600.

Kim J, Tsien RW, Alger BE. 2012. An improved test for detecting multiplicative homeostatic synaptic scaling. PLoS One 7:1–9.

Liao X, Walters ET. 2002. The use of elevated divalent cation solutions to isolate monosynaptic components of sensorimotor connections in Aplysia. J Neurosci Methods 120:45–54.

Lisman J, Schulman H, Cline H. 2002. The molecular basis of CaMKII function in synaptic and behavioural memory. Nat Rev Neurosci 3:175–190.

Mckinney RA, Debanne D, Gahwiler BH, Thompson SM, Gähwiler BH. 1997. Lesion-induced axonal sprouting and hyperexcitability in the hippocampus in vitro: Implications for the genesis of posttraumatic epilepsy. Group 3:990–6.

Miller KD, MacKay DJC. 1994. The Role of Constraints in Hebbian Learning. Neural Comput 6:100–126.

O'Brien RJ, Kamboj S, Ehlers MD, Rosen KR, Fischbach GD, Huganir RL. 1998. Activity-dependent modulation of synaptic AMPA receptor accumulation. Neuron 21:1067–1078.

Ranson A, Cheetham CEJ, Fox K, Sengpiel F. 2012. Homeostatic plasticity mechanisms are required for juvenile, but not adult, ocular dominance plasticity. Proc Natl Acad Sci U S A 109:1311–1316.

Rudy B, Fishell G, Lee S, Hjerling-Leffler J. 2011. Three groups of interneurons account for nearly 100% of neocortical GABAergic neurons. Dev Neurobiol 71:45–61.

Sanhueza M, Fernandez-Villalobos G, Stein IS, Kasumova G, Zhang P, Bayer KU, Otmakhov N, Hell JW, Lisman J. 2011. Role of the CaMKII/NMDA receptor complex in the maintenance of synaptic strength. J Neurosci 31:9170–8.

Shen K, Meyer T. 1999. Dynamic control of CaMKII translocation and localization in hippocampal neurons by NMDA receptor stimulation. Science (80-) 284:162–166.

Shen K, Teruel MN, Connor JH, Shenolikar S, Meyer T. 2000. Molecular memory by reversible translocation of calcium/calmodulin-dependent protein kinase II. Nat Neurosci 3:881–886.

Shin SM, Zhang N, Hansen J, Gerges NZ, Pak DTS, Sheng M, Lee SH. 2012. GKAP orchestrates activity-dependent postsynaptic protein remodeling and homeostatic scaling. Nat Neurosci 15:1655–66.

Sivaramakrishnan S, Sanchez JT, Grimsley CA. 2013. High concentrations of divalent cations isolate monosynaptic inputs from local circuits in the auditory midbrain. Front Neural Circuits 7:175.

Soares C, Lee KF, Nassrallah W, Beique JC. 2013. Differential Subcellular Targeting of Glutamate Receptor Subtypes during Homeostatic Synaptic Plasticity. J Neurosci 33:13547–13559.

Stuchlik A. 2014. Dynamic learning and memory, synaptic plasticity and neurogenesis: an update. Front Behav Neurosci 8:106.

Sutton MA, Ito HT, Cressy P, Kempf C, Woo JC, Schuman EM. 2006. Miniature Neurotransmission Stabilizes Synaptic Function via Tonic Suppression of Local Dendritic Protein Synthesis. Cell 125:785–799.

Sweatt JD. 2016. Dynamic DNA methylation controls glutamate receptor trafficking and synaptic scaling. J Neurochem 137:312–330.

Szczot M, Wojtowicz T, Mozrzymas JW. 2010. Gabaergic and glutamatergic currents in hippocampal slices and neuronal cultures show profound differences: A clue to a potent homeostatic modulation. J Physiol Pharmacol 61:501–506.

Takeuchi T, Duszkiewicz AJ, Morris RGM. 2014. The synaptic plasticity and memory hypothesis: encoding, storage and persistence. Philos Trans R Soc Lond B Biol Sci 369:20130288.

Thiagarajan TC, Piedras-Renteria ES, Tsien RW. 2002. α- and βCaMKII: Inverse regulation by neuronal activity and opposing effects on synaptic strength. Neuron 36:1103–1114.

Turrigiano GG. 2008. The Self-Tuning Neuron: Synaptic Scaling of Excitatory Synapses. Cell 135:422–435.

Turrigiano GG, Leslie KR, Desai NS, Rutherford LC, Nelson SB. 1998. Activity-dependent scaling of quantal amplitude in neocortical neurons. Nature 391:892–896.

Turrigiano GG, Nelson SB. 2000. Hebb and homeostasis in neuronal plasticity. Curr Opin Neurobiol 10:358–364.

Turrigiano GG, Nelson SB. 2004. Homeostatic Plasticity in the Developing Nervous System. Nat Rev Neurosci 5:97–107.

Umemiya M, Senda M, Murphy TH. 1999. Behaviour of NMDA and AMPA receptor-mediated miniature EPSCs at rat cortical neuron synapses identified by calcium imaging. J Physiol 521 Pt 1:113–22.

Verbich D, Becker D, Vlachos A, Mundel P, Deller T, McKinney RA. 2016. Rewiring neuronal microcircuits of the brain via spine head protrusions--a role for synaptopodin and intracellular calcium stores. Acta Neuropathol Commun 4:38.

Vergara PI. 2016. Escalamiento sináptico homeostático rápido en rebanadas agudas de hipocampo (Undergraduate dissertation). Retrived from Bibl Digit Univ Chile (Shelf number UCH-FC Biotecnol V494).

Vest RS, Davies KD, O'Leary H, Port JD, Bayer KU. 2007. Dual Mechanism of a Natural CaMKII Inhibitor. Mol Biol Cell 19:308–317.

Vivès E, Brodin P, Lebleu B. 1997. A truncated HIV-1 Tat protein basic domain rapidly translocates through the plasma membrane and accumulates in the cell nucleus. J Biol Chem 272:16010–16017.

Vlachos A, Becker D, Jedlicka P, Winkels R, Roeper J, Deller T. 2012. Entorhinal denervation induces homeostatic synaptic scaling of excitatory postsynapses of dentate granule cells in mouse organotypic slice cultures. PLoS One 7.

Wang CC, Held RG, Chang SC, Yang L, Delpire E, Ghosh A, Hall BJ. 2011. A critical role for gluN2B-containing NMDA receptors in cortical development and function. Neuron 72:789–805.

Wang CC, Held RG, Hall BJ. 2013. SynGAP regulates protein synthesis and homeostatic synaptic plasticity in developing cortical networks. PLoS One 8.

Watt AJ, van Rossum MCW, MacLeod KM, Nelson SB, Turrigiano GG. 2000. Activity coregulates quantal AMPA and NMDA currents at neocortical synapses. Neuron 26:659–670.

Yashiro K, Philpot BD. 2008. Regulation of NMDA receptor subunit expression and its implications for LTD, LTP, and metaplasticity. Neuropharmacology 55:1081–1094.